



## The new insight into dynamic crossover in glass forming liquids from the apparent enthalpy analysis

Julio Cesar Martinez-Garcia, Jorge Martinez-Garcia, Sylwester J. Rzoska, and Jürg Hulliger

Citation: *The Journal of Chemical Physics* **137**, 064501 (2012); doi: 10.1063/1.4739750

View online: <http://dx.doi.org/10.1063/1.4739750>

View Table of Contents: <http://scitation.aip.org/content/aip/journal/jcp/137/6?ver=pdfcov>

Published by the [AIP Publishing](#)



## Re-register for Table of Content Alerts

Create a profile.



Sign up today!



# The new insight into dynamic crossover in glass forming liquids from the apparent enthalpy analysis

Julio Cesar Martinez-Garcia,<sup>1</sup> Jorge Martinez-Garcia,<sup>2</sup> Sylwester J. Rzoska,<sup>3,4</sup> and Jürg Hulliger<sup>1</sup>

<sup>1</sup>Department of Chemistry and Biochemistry, University of Berne, Freiestrasse 3, CH-3012 Berne, Switzerland

<sup>2</sup>Department of Materials ETH, CH-8093 Zürich, Switzerland

<sup>3</sup>Institute of Physics, University of Silesia, Uniwersytecka 4, 40-007 Katowice, Poland

<sup>4</sup>Institute of High Pressure Physics PAS, Sokółowska 27/39, 00-142 Warsaw, Poland

(Received 22 February 2012; accepted 16 July 2012; published online 8 August 2012)

One of the most intriguing phenomena in glass forming systems is the dynamic crossover ( $T_B$ ), occurring well above the glass temperature ( $T_g$ ). So far, it was estimated mainly from the linearized derivative analysis of the primary relaxation time  $\tau(T)$  or viscosity  $\eta(T)$  experimental data, originally proposed by Stickel *et al.* [J. Chem. Phys. **104**, 2043 (1996); J. Chem. Phys. **107**, 1086 (1997)]. However, this formal procedure is based on the general validity of the Vogel-Fulcher-Tammann equation, which has been strongly questioned recently [T. Hecksher *et al.* Nature Phys. **4**, 737 (2008); P. Lunkenheimer *et al.* Phys. Rev. E **81**, 051504 (2010); J. C. Martinez-Garcia *et al.* J. Chem. Phys. **134**, 024512 (2011)]. We present a qualitatively new way to identify the dynamic crossover based on the apparent enthalpy space ( $H'_a = d \ln \tau / d(1/T)$ ) analysis via a new plot  $\ln H'_a$  vs.  $1/T$  supported by the Savitzky-Golay filtering procedure for getting an insight into the noise-distorted high order derivatives. It is shown that depending on the ratio between the “virtual” fragility in the high temperature dynamic domain ( $m_{\text{high}}$ ) and the “real” fragility at  $T_g$  (the low temperature dynamic domain,  $m = m_{\text{low}}$ ) glass formers can be splitted into two groups related to  $f < 1$  and  $f > 1$ , ( $f = m_{\text{high}}/m_{\text{low}}$ ). The link of this phenomenon to the ratio between the apparent enthalpy and activation energy as well as the behavior of the configurational entropy is indicated. © 2012 American Institute of Physics. [<http://dx.doi.org/10.1063/1.4739750>]

## I. INTRODUCTION

The underlying origin of the glass transition is considered as one of great challenges of the modern condensed matter physics and the material science at the beginning of the 21st century.<sup>1–4</sup> Its most surprising feature is an extraordinary increase of viscosity ( $\eta$ ) or structural (primary) relaxation time ( $\tau$ ) by 15 decades taking place above the glass temperature ( $T_g$ ), for  $(T_m - T_g)/T_g < 0.3$  ( $T_m$  is for the melting temperature).<sup>1–7</sup> The parameterization of  $\eta(T)$  or  $\tau(T)$  behavior in the supercooled domain is still the basic artifact in searching for the ultimate theoretical model.<sup>4,5,7</sup> This is supported, by surprisingly universal behavior seen in  $\log_{10}\eta$  or  $\log_{10}\tau$  vs.  $T_g/T$  plots, with the metric known as the fragility and being defined as:<sup>7,9</sup>

$$m = m_P(T \rightarrow T_g) = \left[ \frac{d \log_{10} x(T)}{d(T_g/T)} \right]_{T \rightarrow T_g}, \quad (1)$$

where the function  $x(T)$  is for  $\eta(T)$  or  $\tau(T)$  experimental data ( $T > T_g$ ), the index “ $P$ ” stays for the isobaric steepness index  $m_P(T)$ . It is assumed that  $\tau(T_g) = 100$  s,  $\eta(T_g) = 10^{13}$  P and the fragility is defined as the steepness index  $m_P(T)$  at  $T = T_g$ .

The vitrification is essentially a kinetic phenomenon and consequently the value of the glass temperature depends on the rate of cooling.<sup>7</sup> Notwithstanding, the fact that pre-vitrification phenomena appear well above  $T_g$  it shows some similarities to pretransitional anomalies on approaching a continuous phase transition.<sup>10,11</sup> The most classical way

of parameterization of  $\tau(T)$  or  $\eta(T)$  behavior is the Vogel-Fulcher-Tammann (VFT) equation, namely,<sup>4–12</sup>

$$\tau(T) = \tau_0 \exp \left( \frac{D_T T_0}{T - T_0} \right) \quad \text{for } T > T_g, \quad (2)$$

where  $T_0 \ll T_g$  denotes the VFT estimation of the “ideal” glass transition: most often  $T_0 = T_g - (30 \div 40 \text{ K})$ ,  $D_T$  is the fragility strength coefficient which is considered as an alternative measure of fragility:  $m = m_{P=0.1 \text{ MPa}} \approx 16 + 590/D_T$ , for  $T = T_g$ .

For strongly non-Arrhenius dynamics (*fragile* glass formers)  $m = m_P(T \rightarrow T_g)$  is large and  $D_T$  is small, whereas the opposite takes place for the near-Arrhenius behavior (*strong* glass formers). Although the VFT equation is essentially empirical, it can also be derived from some basic theoretical models for the glass transition physics.

One of the most important models, proposed by Doolittle<sup>13</sup> and later extended by Greet and Turnbull,<sup>14</sup> is associated with the free volume approach. They assumed that molecules in the supercooled state need a “free” volume  $v_f(T)$  to rearrange what finally lead to the equation:<sup>13,14</sup>

$$\tau(T) = \tau_0 \exp \left( \frac{B}{v_f/v_g} \right), \quad (3)$$

where  $v_f$  is for apparent free volume and  $v_g$  denotes the volume at the glass transition. For  $v_f/v_g = \chi_T(T - T_0)$  ( $\chi_T$  is the isothermal compressibility) the VFT equation can be recovered. The hypothetically universal empirical

value of the activation coefficient  $B$  was suggested to be  $0.9 \pm 0.3$ .<sup>14</sup>

Another important model was introduced by Adam and Gibbs (AG) who invoked the concept of cooperatively rearranging regions (CRRs), being defined as the smallest volume changing its configuration independently from neighbouring regions.<sup>15</sup> As the temperature is lowered CRRs are growing and consequently:<sup>15</sup>

$$\tau(T) = \tau_0 \exp\left(\frac{A\Delta\mu}{TS_C}\right), \quad (4)$$

where  $\Delta\mu$  is defined as the conventional free energy barrier to rearrangement,  $S_C$  the excess (configurational) entropy of the Kauzmann paradox, which itself depends on the value of the configurational heat capacity  $S_C = \Delta C_P \ln T/T_K$ , and  $A$  is a constant. Assuming  $\Delta C_P = K/T$ ,  $S_C(T) = K(T - T_K)/TT_K$  is obtained, yielding the VFT equation for the case of  $T_0 = T_K$ . The temperature  $T_K$  is termed as the Kauzmann temperature and defines a limit where the entropy of the liquid state by extrapolation can become lower than that of the crystal.

More than a decade ago, Stickel *et al.*,<sup>16,17</sup> indicated that the validity of VFT description in supercooled glass forming liquids is associated with the linearity at  $\varphi_T = [\log_{10} \tau / d(1/T)]^{-1/2}$  vs.  $1/T$  plot. In subsequent years, it became a key tool for estimating the so-called dynamic crossover temperature  $T_B$  between two dynamic domains.<sup>7,18–24</sup> It was shown that at least two VFT equations are desired for describing pre-vitrificational slowing down in a broader range of temperatures. The temperature  $T_B$  has been also recognized as a milestone in the way on approaching  $T_g$  since a lot of exceptional phenomena disclose there, for instance:<sup>18–31</sup> (1) the loss of ergodicity as predicted by mode-coupling theory (MCT), (2) increasing broadening of the structural relaxation time distribution, (3) a marked change in temperature dependence of the nanopore unoccupied volume radius, (4) splitting of the high temperature relaxation into the primary and secondary relaxation times, (5) orientational-translational decoupling, (6) for a broad set of supercooled systems  $\tau(T_B) = 10^{-7 \pm 1}$  s or  $\eta(T_B) \approx 10^3$  P- i.e., it is near-universal, (7)  $\tau(T_B, P_B)$ ,  $\eta(T_B, P_B) = \text{const}$  for a given glass former, (8) it is believed that the dynamical crossover is closely related to the onset of caging and appearing of dynamical heterogeneities, (9) the coefficient  $D_T$  in the VFT equation almost always increases on crossing to the dynamical domain in the immediate vicinity of  $T_g$ . The latter may indicate that always a fragile (F) to less fragile or strong (S) transformation when passing  $T_B$  occurs. This process is associated with the permanent increase of the steepness index, which finally at the glass temperature may reach values linked to the fragile pattern ( $m > 30$ ).<sup>22</sup> These facts are worth stressing because the dynamic crossover is sometimes linked to the “FS” crossover.<sup>32</sup>

However, there are fundamental weak points in the discussion employing the “Stickel analysis” carried out so far, namely: (1) an impressive number of papers discussing the dynamical crossover explores only the “formal” plot  $\varphi_T$  vs.  $1/T$ , or its pressure counterpart  $\varphi_P = (d \log_{10} \tau / dP)^{-1/2}$  vs.  $P$ ,

without an attempt of finding a possible physical meaning hidden behind<sup>18–33</sup> (2) the general validity of the VFT equation, underlying  $\varphi_T(T)$  “Stickel” function, has been strongly questioned in recent years.

Regarding the latter, it is advised that VFT parameterization may lack the physical meaning: Tanaka *et al.*<sup>34</sup> reported a compilation of experimental data showing that the identification  $T_0 = T_K$  is not confirmed by experiments. Even stronger conclusion was pointed out by the theoretical analysis of Eckmann and Procaccia,<sup>35</sup> who explicitly demonstrated that the configurational entropy is finite at any temperature and concluded that the Kauzmann temperature may not exist. Hecksher *et al.*,<sup>5</sup> collected 42 sets of  $\tau(T)$  experimental data in supercooled liquids and performed a fitting comparison between the VFT, Avramov-Bässler (AB),  $\tau(T) = \tau_0 \exp(B/T^n)$  and two other formal equations without a finite temperature divergence.<sup>36,37</sup> It was concluded that there are no compelling evidence justifying the dominance of the VFT description for describing dynamics in supercooled liquids.

Recently, to overcome these problems, Mallamace *et al.*<sup>32</sup> advised to explore the MCT critical-like equation (discussed briefly below) for estimating  $T_B$ .

Very recently, Mauro *et al.*<sup>38</sup> employed the constraint theory to the Adam–Gibbs model basic Eq. (4) and obtained the relation earlier introduced empirically by Waterton<sup>39</sup> in 1932.

The application of the Waterton–Mauro equation (WM),<sup>38,39</sup> showed its superior fitting quality in comparison to VFT and AB parameterizations. It is noteworthy that the WM equation does not exhibit a finite temperature singularity below  $T_g$ , which is the key feature of the VFT relation,<sup>23,40</sup> underlying the “Stickel linearization.”

The basic importance of the dynamic crossover was recently concluded in Ref. 32: “... one may expect that understanding the meaning of the dynamic crossover phenomenon may be essential for the ultimate understanding of the puzzling nature of the glass transition. ...,  $T_B$  appears to be more relevant than  $T_g$  or  $T_0$  ...”

This statement can be strengthened by several fundamental theoretical and simulation studies which have suggested a change in the nature of the dynamics of supercooled fluids, leading to the concept of a dynamic crossover as a milestone point on the way towards the glass transition. The review of these studies, focusing on molecular dynamics approach, was given by Anderssen,<sup>41</sup> who indicated also serious limitations associated with understanding the meaning of the crossover. Hence, also from this point of view, novel results regarding the dynamic crossover phenomenon can be of basic importance.

This paper presents new investigations of the dynamic crossover phenomenon which explore the apparent enthalpy space properties. Reasoning is supported by the analysis of  $\tau(T)$  data for 27 supercooled glass forming systems, including low molecular weight liquids, polymeric liquid and hardly discussed liquid crystals and orientationally disordered crystals. Two questions are focused: How to determine the dynamic crossover beyond the VFT equation? What is the physical meaning of the dynamic crossover hidden behind?

## II. APPARENT ACTIVATION ENTHALPY ANALYSIS

In recent years, novel equations yielding more optimal parameterizations of  $\tau(T)$  or  $\eta(T)$  experimental data, and questioning the general validity of the VFT relation, appeared.<sup>5,25,38,39</sup> Particularly, noteworthy seems to be the Waterton-Mauro (MW) equation<sup>38,39</sup> which validity has been regained recently.<sup>23,38,40</sup>

$$\tau(T) = \tau_0 \exp \left[ \frac{K}{T} \exp \left( \frac{C}{T} \right) \right]. \quad (5)$$

It is worth stressing that it has no final temperature divergence, which is characteristic for the VFT dependence. Notwithstanding, for selected types of glass formers, such as liquid crystals or orientationally disordered crystals, an ultimate prevalence for the critical-like parameterization was proved, namely,<sup>10,22,23,54</sup>

$$\tau(T) = \tau_0 \left( \frac{T - T_C}{T_C} \right)^{-\phi}, \quad T_C < T_g \quad (6)$$

where the exponent  $\phi \rightarrow 9$ , in fair agreement with dynamical scaling model (DSM) predictions. Most often  $T_C \approx T_g - 10$  K.

It is noteworthy that an analogous equation holds in the high temperature domain of probably all supercooled systems. In this case the power exponent is in fair agreement with the MCT predictions ( $\phi = 1.4 \div 4$ ) and  $T > T_C = T_C^{MCT} + \Delta T$  ( $\approx 20$  K),  $T_C \ll T_g$ .<sup>10,22,23</sup> The empirical coincidence between  $T_B$  and  $T_C^{MCT}$  is commonly accepted. Most often for estimating  $T_C^{MCT}$  directly from Eq. (6), for instance via the plot  $(\ln \tau)^{1/\phi}$  or  $(\ln \eta)^{1/\phi}$  vs.  $T$  is used.<sup>22,23,62</sup> However, as indicated in Ref. 22, such analysis can lead to an impressing error due to the very large value of  $\Delta T$ . This problem can be overcome employing the linearized enthalpy-space and derivative-based analysis.<sup>22</sup>

Regarding the physical meaning of the “Stickel function”<sup>16,17</sup>  $\varphi_T$  it is worth recalling that generally the non-Arrhenius behavior can be described by the “apparent” Arrhenius function:<sup>7</sup>

$$\tau(T) = \tau_0 \exp \left( \frac{E_a(T)}{RT} \right). \quad (7)$$

The general form of the evolution of the activation energy  $E_a(T)$  is unknown, but the first derivative of Eq. (7) yields:<sup>22</sup>

$$\frac{d \ln \tau}{d(1/T)} = \frac{H_a(T)}{R} = H'_a = T m_P / \log_{10} e, \quad (8)$$

where  $R$  denotes the gas constant and  $H_a(T)$  stands for the apparent activation enthalpy.

Using the VFT Eq. (2) one obtains:<sup>22,23</sup>

$$(H'_a)^{-1/2} = [(D_T T_0)^{-1/2}] - \frac{[T_0(D_T T_0)^{-1/2}]}{T} = A - \frac{B}{T}. \quad (9)$$

This relation recalls the  $\varphi_T(T)$  “Stickel function”:<sup>16,17</sup> since  $\ln \tau = \log_{10} \tau / \log_{10} e$ . Consequently, both plots  $\varphi_T$  and  $(H'_a)^{-1/2}$  vs.  $1/T$  are linked to the evolution of the apparent enthalpy and are shadowed by the hypothetical validity of VFT

equation.<sup>22,23</sup> In each case, the region of the validity of the VFT equation is indicated by linear domains, for which the linear regression analysis yields optimal values of the basic parameters,  $T_0 = B/A$  and  $D_T = 1/AB$ , prior to  $\tau(T)$  ultimate fitting via the VFT equation.<sup>22</sup>

It is noteworthy that a linearized derivative-based linearized approached can also be developed for the WM equation, namely,<sup>23</sup>

$$\ln \left[ \frac{H'_a}{1 + C/T} \right] = \ln K + \frac{C}{T}. \quad (10)$$

For the optimal selection of  $C$  constant, a linear dependence at the plot  $\ln[H'_a/(1 + C/T)]$  vs.  $1/T$  will show the domain of the validity of the WM equation.<sup>23</sup> The experimental evidence revealed the manifestation of the dynamical crossover via the inflection point also at such plot. Its loci appeared to approximately independent from the value of  $C$  and then for estimation of  $T_B$  a simple plot  $\ln H'_a$  vs.  $1/T$  can be used.<sup>23,42</sup>

## III. ON THE NEW PLOT

For discussing the new plot it is important to clarify the difference between the apparent activation enthalpy and activation energy. The latter  $E'_a(T) = E_a(T)/R = T \ln(\tau/\tau_0)$  cannot be estimated from the derivative of  $d \ln \tau / d(1/T)$ , which determines the activation enthalpy.<sup>22</sup> From Eq. (7) we can easily demonstrate that

$$H'_a(T) = E'_a(T) \left[ 1 + \frac{1}{T} \frac{\partial \ln(E'_a(T))}{\partial(1/T)} \right]. \quad (11)$$

Assuming the validity of the AG model equation  $E'_a(T) \propto C/S_C(T)$  one can show further the link to the configurationally entropy

$$H'_a(T) = E'_a(T) \left[ 1 - \frac{1}{T S_C(T)} \frac{\partial S_C(T)}{\partial(1/T)} \right] = E'_a(T) \delta(T) \quad (12)$$

and

$$\frac{\partial \ln(H'_a(T))}{\partial(1/T)} \propto \frac{\partial \ln(E'_a(T))}{\partial(1/T)} = - \frac{1}{T S_C(T)} \frac{\partial S_C(T)}{\partial(1/T)}. \quad (13)$$





























The latter relation means that slope  $a(T) = d \ln H'_a / d(1/T)$  at  $\ln H'_a$  vs.  $1/T$  graph can be defined by the solution of the differential equation of the configurationally entropy, namely,

$$\frac{\partial S_C(T)}{\partial(1/T)} + a(T) S_C(T) = 0. \quad (14)$$

The same configurational entropy equation was obtained by the energy landscape analysis of Naumis<sup>43</sup> and the temperature-dependent constraint model of Gupta and Mauro.<sup>44</sup> It can be recovered for constant values of  $a(T)$ . Materials with dynamical crossover can be ascribed by a departure from the constant slope  $a(T)$ .

On the other hand, considering directly the AG model via Eq. (4) and the free volume via Eq. (3), one can interrelate the

TABLE I. The set of glass forming systems used in the analysis, including its symbol abbreviation, temperature interval in which  $\tau(T)$  data were available RT[K], frequency interval for the dielectric loss measurements determining the relaxation times ( $R\log_{10}\nu$ ) and source references.

Supercooled, glass forming system	Abbr.	Symbol	RT(K)	$R\log_{10}\nu$	Ref.
Cresolphthalein-dimethylether	KDE		311; 504	-1.46; 10.38	50
Polyvinylacetate (PVac)167	(PVac)a		311; 355	-1.20; 5.64	51
Polyvinylacetate (PVac)170	(PVac)c		307; 463	-2.03; 10.07	52
Polyvinylacetate(PVAc)15	(PVac)d		301; 446	-0.85; 9.54	53
Polyvinylacetate (PVAc)15	(PVac)b		288; 464	-6.34; 9.30	55
Polychlorinatedbiphenyl (62%)	PCB62		261; 376	-2.62; 9.66	55
Polychlorinatedbiphenyl (54%)	PS540		258; 337	-0.30; 8.41	56
Epoxy resins bisphenol	EPON828		258; 340	-1.30; 9.58	57
Xylitol	Xyl		243; 400	-2.76; 11.26	58
Polychlorinatedbiphenyl (54%)	PCB54		249; 363	-0.77; 9.95	55
O-terphenyl	OTP		243; 368	-1.13; 11.70	59
Isooctylcyanobiphenyl	8*OCB		224; 413	-0.11; 10.13	60
Polychlorinatedbiphenyl (42%)	PCB42		220; 328	-1.40; 10.07	55
Phenyl-salicylate (salol)	Sal		219; 430	-0.79; 11.26	16
Isopentylcyanobiphenyl	5*CB		236; 438	4.39; 9.91	61
5CB+7CB+80CB+5CT (LC eutectic mixture)	E7		210; 386	-0.33; 8.56	10
Glycerol	Gly		196; 343	-0.74; 8.56	62
Tripolypropylene-glycol	triPPG		190; 340	-1.22; 10.85	40
Dipolypropylene-glycol	dIPPG		195; 323	-0.73; 8.91	62
Diethyl-phtalate	DEP		187; 292	0.86; 10.54	63
Di-iso-butyl-phtalate	dIBP		183; 293	-0.61; 8.60	64
Polypropylene-glycol	PPG		175; 353	-0.91; 9.61	62
Neopentylalcohol-neopentylglycol (32%)	NPANPG		161; 370	-1.15; 10.40	64
Propylene carbonate	PC		159; 370	0.17; 11.70	53
Cycloheptanol- cyclooctanol(26%)	C8C7		155; 233	-0.34; 6.64	65
Ethanol	Eth		96; 250	-2.75; 9.86	66
2-Methyl-tetrahydrofuran	MTHF		91; 180	-0.10; 11.76	46, 67
Di-clorodifluometano (freon12)	f12		90; 159	-0.36; 10.59	68

configuration entropy and the free volume

$$S_C(T) = A \frac{1}{T} v_f(T), \quad (15)$$

where  $A$  is a constant.

Relations (13) and (15) lead to

$$a(T) = - \left( T + \frac{1}{v_f(T)} \frac{dv_f(T)}{d(1/T)} \right) = T(T\alpha_f - 1). \quad (16)$$

Consequently, the tangent at  $\ln H'_a$  vs.  $1/T$  plot can also be associated with the change of the free volume thermal expansion coefficient  $\alpha_f = (1/v_f)(\partial v_f/\partial T)$ .

## IV. RESULTS AND DISCUSSION

In the given paper we consider 27 sets of  $\tau(T)$  data for supercooled glass forming systems, which are presented in Table I. Explicit the way of treatment of experimental data is discussed for supercooled *phenyl-salicylate* (Salol) (Ref. 45) and 2-methyl-tetrahydrofuran (MTHF).<sup>46</sup>

For the analysis essentially important were higher order derivatives of  $\ln \tau(1/T)$ . However, they are strongly influenced by the noise distortion, limiting reliable conclusions appearing due to the experimental error.<sup>5</sup> To overcome this fundamental problem, we used the Savitzky-Golay (SG) filtering procedure.<sup>47,48</sup> It is based on the fitting of a subgroup data point are  $n = 2m + 1$  integer with  $m$  positive integer from 1



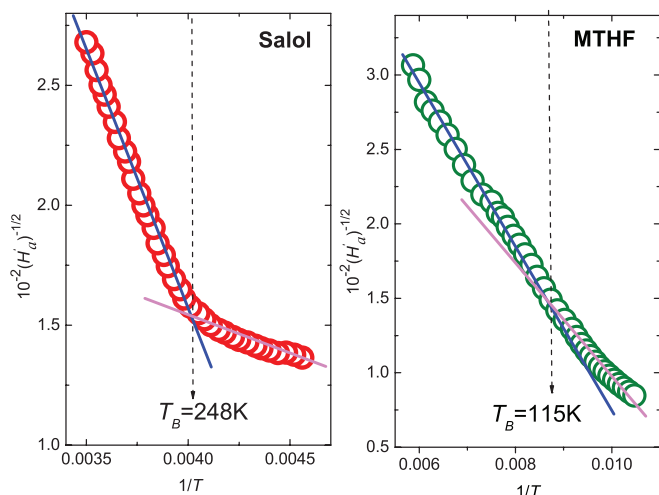


FIG. 1. The derivative based analysis of primary relaxation time  $\tau(T)$  for (Salol) and (MTHF) data. Lines indicate domains of the validity of the VFT parameterization and the linear regression fit estimates the optimal values of  $D_T$  and  $T_0$  (see Eq. (9) and Ref. 22). Note that the same pattern of the temperature evolution occurs for both compounds. The simple Arrhenius behavior domain should appear as a horizontal line. Note that the crossover temperature from the “Stickel-type”<sup>16,17,22</sup> analysis is denoted by  $T_B$ .

to 12, to a polynomial of degree  $p$  ( $p \leq 2m$ ) in the last-squares series:

$$\frac{\partial}{\partial b_k} \left[ \sum_{i=-m}^{i=m} \left( \sum_{k=0}^n b_k i^k - y_i \right)^2 \right] = 0. \quad (17)$$

It converts each points of this subgroups to temporary coordinate system in which the ordinate values range from  $i = -m$  to  $i = m$ , where the midpoint is defined as  $i = 0$ . All the data within the window is used to perform a least square fit of Eq. (17), but only the central point is smoothed for each window position. It allows a reduction of the experimental noise keeping its higher moments. Consequently, it provides a way for obtaining the dominated functional behaviour of noise-distorted derivatives.

Figure 1 shows results of the derivative-based analysis of the primary relaxation time for Salol and MTHF, focusing on the hypothetical validity of the VFT parameterization, via Eqs. (2) and (9). For both compounds the same pattern of behavior occurs, namely, the increase of  $D_T$  parameter in the VFT equation on moving from the high to the low temperature dynamical domain. This can suggest that, a supercooled liquid is stronger (less fragile) in the dynamical domain close to  $T_g$ . However, parallel the steepness index  $m_p(T)$  increases continuously on approaching  $T_g$ . The comparison with a large number of “Stickel plots” available in the literature<sup>7,18–36</sup> indicates that this is a typical pattern for glass formers which have been tested so far.

Figure 2 focuses on the estimation of the dynamic crossover appearing in the derivative-based plot  $\ln H'_a$  vs.  $1/T$ , where  $H'_a = d \ln H'_a / d(1/T)$ . The coincidence between loci of the dynamic crossover ( $T'_B$  and  $T_B$ ) obtained via plots presented in Figs. 1 and 2 is clearly visible in Fig. 3. It also confirms the mentioned coincidence between the dynamic crossover temperature ( $T'_B$ ) and the MCT “critical-like tem-

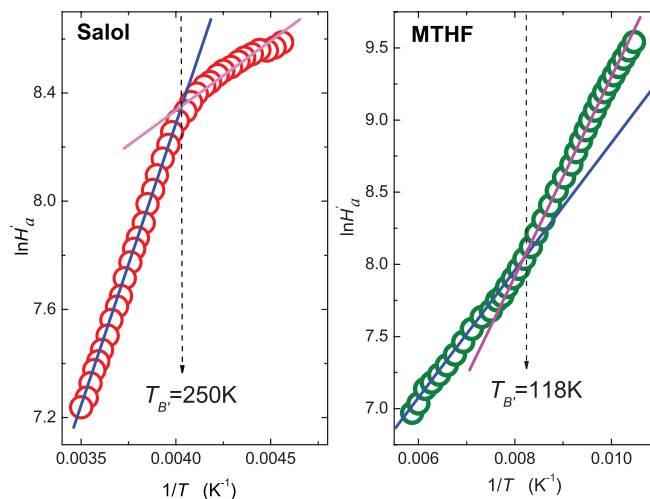


FIG. 2. The derivative based analysis of  $\tau(T)$  data exploring the novel plot, recalling the Waterton-Mauro dependence (Eq. (10) and Ref. 23). Note the “down” (Salol) and “up” (MTHF) behavior in the low temperature dynamic domain, near  $T_g$ . Note that the crossover temperature from the new analysis proposed in this paper is denoted by  $T'_B$ .

perature”  $T_C^{MCT}$ . The latter values were precisely estimated via the linearized derivative analysis proposed in Ref. 22.

Values of the dynamic crossover temperature and the glass temperature can be correlated via:  $T'_B = 1.097T_g + 13.47(K)$ .

The ultimate estimation of the dynamical crossover makes possible the analysis related to derivatives of plots presented in Fig. 4. However, they are related to the third derivative of basic  $\tau(T)$  data, and then it they suffer seriously from the consequences of the related experimental error. In practice this artifact causes that reasonable analysis of  $\tau(T)$  data were reduced so far to its second order derivatives.<sup>5</sup>

Notwithstanding, the application of the (SG) filtering procedure enables to obtain reliable output even for highly distorted data, as also shown in Fig. 4. All the data within a window of  $n = 2m + 1$  point is used to perform the least

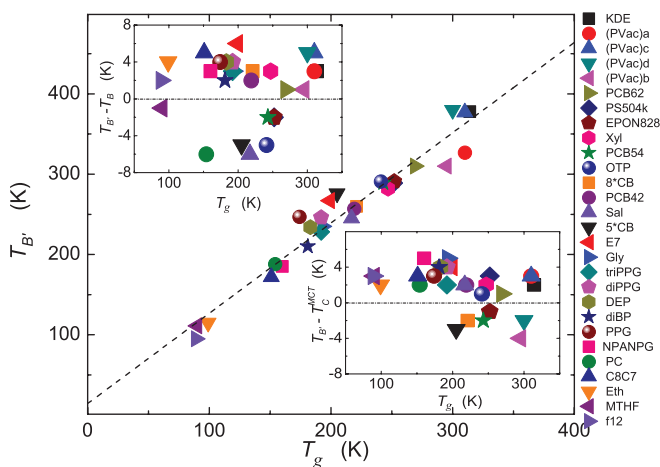


FIG. 3. Correlations of the dynamic crossover temperatures  $T_B$  and  $T'_B$ , calculated with the implementation of the smoothing SG filtering procedure. The lower inset presents the coincidence with the MCT “critical-like” temperature  $T_C^{MCT}$  (see Eq. (6) and comments below).

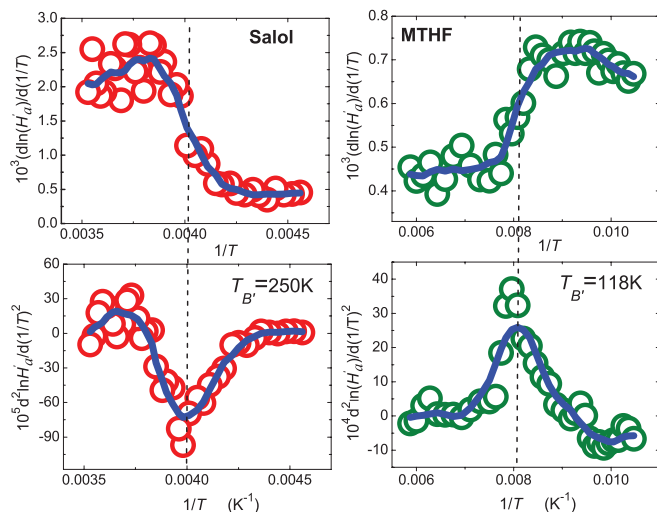


FIG. 4. The derivative based analysis of the  $\ln H'_a$  vs.  $1/T$  dependences from Fig. 3 for supercooled Salol and MTHF. The output results are analysed via the SG smoothing procedure (blue curves which have been obtained for SG parameters  $s = 0$ ,  $p = 3$ ,  $n = 15$ ). The dynamical crossover temperatures  $T_{B'}$  are indicated by dashed lines.

square fit of Eq. (17). In Fig. 4 the blue line represents the curve with ( $s = 0$  (smoothed curve),  $d = 3$  (polynomial order), with filter ( $2m + 1 = 15$ ) points), and 7 point on each side. Our analysis was done by the use Origin 8.0, the reflect boundary condition was used.

This way of analysis was used for estimating the crossover temperatures for the collected compounds showed in Fig. 3. It is worth stressing that Figs. 2 and 4 show different patterns of behavior on passing  $T_{B'}$  for Salol and MTHF (“up” and “down” modes). This feature is not visible for the Stickel-like, VFT based analysis (Fig. 1). Figures 1 and 2 show that there two sets of parameters in a supercooling glass forming liquids, both for VFT or WM equations, in subsequent dynamic domains.

One can consider apart from the real fragility index  $m_{low} = m = m_p(T_g)$  also the virtual fragility index associ-

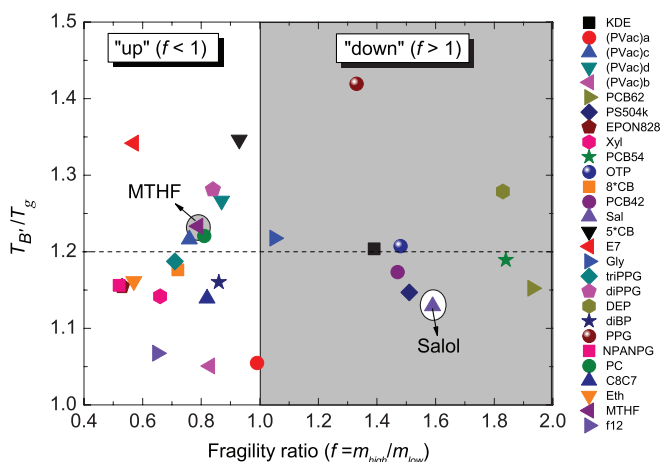


FIG. 5. The relationship between the normalized dynamical crossover temperature and the fragility ratio for the subsequent dynamical domains. The “up” and “down” behaviours are manifested at  $\ln H'_a$  vs.  $1/T$  plot. The parameters  $m_{low} = m = m_p(T_g)$  and  $m_{high} = m_p(T_{g'})$  define the fragilities for the low and high temperature domain around  $T_{B'}$  where  $T_{g'}$  is ascribed to the virtual extrapolated glass temperature and  $T_g$  to real glass temperature.

ated solely for the high temperature dynamical domain system  $m_{high} = m_p(T_{g'})$  and estimate the virtual extrapolated glass temperature  $T_{g'}$ , from the condition  $\tau(T_{g'}) = 100$  s via VFT or MW equations based on the optimal parameters for the high temperature dynamical domain. Consequently, one can introduce the fragility ratio defined as  $f = m_{high}/m_{low}$ . Such factor was in fact already considered by Zhang *et al.*<sup>49</sup> for describing the Fragile-Strong (FS) transition of metallic glass-forming liquids. We noted that only one WM equation was used for describing the previtrification slowing down issue and they did not take in to account the dynamic crossover issue near to  $T_g$ , reporting always values of ( $f$ ) larger than the unity.<sup>49</sup>

Figure 5 presents the normalized dependence of the dynamic crossover temperature  $T_{B'}/T_g$  vs. the fragilities ratio  $f$  for all tested glass forming systems. It reveals the clear link of  $f > 1$  and  $f < 1$  values of the fragilities ratio and to the “up” and “down” behavior near  $T_g$  noted above. The vertical line ( $f = 1$ ) defines the boundary between those groups material. The horizontal line is for  $T_{B'}/T_g \approx 1.2$  often indicated as a typical one, although the dependence of  $T_B$  from the fragility  $m = m_{low}(T_g)$  was also reported.<sup>25,32</sup>

From Eq. (12), one can define a scaling function which can yield an insight into the evolution of the configurational entropy, namely,

$$\delta(T) = T \left( 1 - \frac{H'_a(T)}{E'_a(T)} \right) = \frac{1}{S_C(T)} \frac{\partial S_C(T)}{\partial(1/T)}. \quad (18)$$

This makes it possible to define a new scaling plot as  $\delta(T)/|\delta(T_{B'})|$  vs.  $T_{B'}/T$ , which is presented in Fig. 6. The clear scaling takes place in the high temperature dynamic domain but in the low temperature domain  $T_g < T < T_{B'}$  a split into “up” and “down” modes occur. Figure 6 makes it possible to link this feature to the evolution of the configurational entropy and eventually to the development of CRR–heterogeneities.

The summary of relevant parameters and fitting results is given in Tables I and II. The “Stickel-plot” related crossover

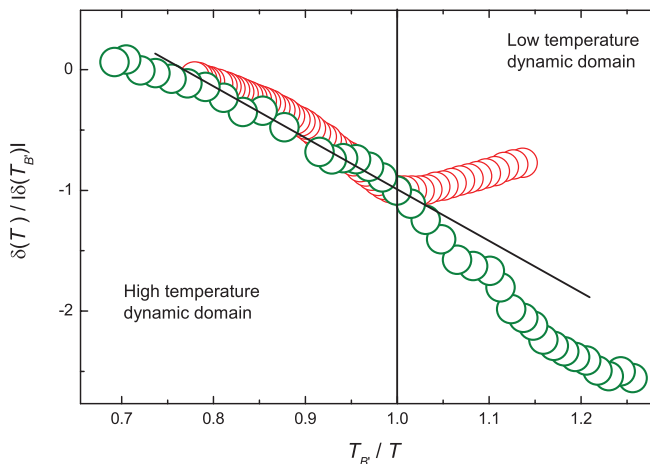


FIG. 6. The scaling plot employing Eq. (18) which is based on  $\tau(T)$  data for Salol (red) and MTHF (green):  $\delta(T) = T(1 - H'_a(T)/E'_a(T)) = (1/S_C)(\partial S_C(T)/\partial(1/T))$  and  $T_{B'} \approx T_B$ ,  $T_C^{MCT}$  is the dynamic crossover temperature. The straight line is a guide for eyes to visualize the “up” and “down” modes for the low temperature dynamic domain close to  $T_g$ .

TABLE II. The dynamic crossover temperature, “real” and virtual glass temperatures and fragilities linked to the high temperature and low temperature dynamic domains.

Liquid	$T_B$ (K)	$T_{B'}$ (K)	$T_C^{MCT}$ (K)	$T_{g'}$ (K)	$m_{high}$	$T_g$ (K)	$m_{low} = m$	$f$
KDE	375	378	380	322	97	314	70	1.29
(PVac)a	324	327	330	309	84	310	85	0.98
(PVac)c	372	377	380	306	74	310	98	0.76
(PVac)d	375	380	378	302	68	295	82	0.83
(PVac)b	309	310	306	296	69	300	79	0.87
PCB62	309	310	311	279	110	268	57	1.93
PS540	291	289	292	255	116	255	77	1.51
EPON 828	293	291	290	240	76	252	142	0.54
Xyl	279	282	284	238	64	247	97	0.66
PCB54	291	289	287	258	112	247	61	1.84
OTP	296	291	292	252	123	243	83	1.48
8*OCB	257	260	258	217	61	221	85	0.72
PCB42	255	257	259	227	99	221	63	1.57
Sal	248	250	247	224	116	218	73	1.59
5*CB	281	276	273	35	52	205	56	0.93
E7	261	267	271	200	47	199	82	0.57
Gly	232	235	240	195	43	194	41	1.05
triPPG	225	228	230	186	55	190	78	0.71
dIPPG	242	246	250	191	48	194	57	0.84
DEP	230	234	238	189	99	179	54	1.83
dIBP	208	210	214	179	54	181	63	0.84
PPG	243	247	250	186	53	175	40	1.33
NPANG	182	185	190	152	34	161	65	0.52
PC	194	188	190	148	73	157	90	0.81
C8C7	167	172	175	149	28	151	34	0.82
Eth	111	115	117	200	47	199	82	0.57
MTHF	115	118	116	84	65	91	82	0.79
fl2	93	95	98	87	53	91	82	0.64

temperature and the MCT “critical temperature” ( $T_{B'}$ ,  $T_C^{MCT}$ ) were obtained by the linearized derivative analysis procedure proposed in Ref. 22. We calculated ( $f$ ) performing two steps of data analysis around the temperature crossovers  $T_{B'}$ . In the first step ( $T > T_{B'}$ ) the optimal fitting parameters for the WM equation were obtained by the enthalpy space analysis procedure.<sup>23</sup> The steepness index  $m_{high} = m_P(T_{g'})$  is calculated by extrapolation up to  $\tau = 100$  s. This parameter is related to the virtual glass transition temperature  $T_{g'}$ . In the second step, ( $T_g < T < T_{B'}$ ), the fitting parameters were obtained by the same procedure, from which the steepness index  $m_P$  is also obtained. Parameters for the low temperature domain, are associated with the real glass transition temperature  $T_g$ . The crossover temperature  $T_{B'}$ , was calculated by the inflexion point of the second derivative of the smoothed curves of  $\ln H'_a$  vs  $1/T$  plot.

## V. OUTLOOK

Concluding, the significance of the dynamical crossover temperature  $T_B$  was first noted when testing the validity of the VFT equation via the plot of the “Stickel function.”<sup>16,17</sup> Since then, it was identified as the onset of variety of dynamical phenomena, which are fundamental for the final vitrification occurring at  $T_g$ . This paper indicates that the dynamic crossover loci can be estimated also behind the VFT equation via the plot  $\ln H'_a(1/T)$ , supported by its derivatives. The obtained

values of  $T_{B'}$  correlate with  $T_C^{MCT}$  and may indicate a possible link between the dynamic crossover and a hypothetical hidden phase transition. The proposed analysis also revealed a possible existence of two general patterns of the dynamic crossover unknown so far, which can be distinguished as “up” or “down” groups of glassy materials. We showed also that the configurational entropy equation introduced by Mauro,<sup>38</sup> cannot be used in all temperature dynamic domains for describing the dynamic of the supercooled state. For materials with the dynamic crossover, a more general equation is needed. It is also noted that the tangent at  $\ln H'_a$  vs.  $1/T$  plot can be associated with the change of the free volume thermal expansion coefficient. Taking into account results of Ref. 69, one can relate the apparent enthalpy to the number of molecules in the CRR as  $d \ln H'_a / d(1/T) \propto N_C^{1/2}(T)$ . Finally, we would like to stress the significance of the analysis in the apparent enthalpy space and the possible significance for the Savitzky-Golay smoothing/filtering procedure<sup>47,48</sup> which made it possible, to withdraw information even from the third derivative (!) of dielectric relaxation time or viscosity experimental data.

## ACKNOWLEDGMENTS

S. J. Rzoska was supported by the National Centre for Science (NCN, Poland) (Grant No. N N202 231737). The



authors are very grateful to all authors recalled for superior experimental data. J.C.M.-G. would like to thank Professor Dr. Jose Luis Tamarit Mur for introducing him in the past into the glass transition and ODIC topics.

- <sup>1</sup>P. W. Anderson, "Through the glass lightly," *Science* **267**, 1616 (1995).
- <sup>2</sup>K. Chang, "The nature of glass remains anything but clear," *The New York Times*, July 29, 2008.
- <sup>3</sup>*Science* **309**, 83 (2005), "125th Anniversary Issue: 125 outstanding problems in all of science," available at <http://www.sciencemag.org/site/feature/misc/webfeat/125th/>.
- <sup>4</sup>S. A. Kivelson and G. Tarjus, *Nature Mater.* **7**, 831 (2008).
- <sup>5</sup>T. Hecksher, A. I. Nielsen, N. B. Olsen, and J. C. Dyre, *Nature Phys.* **4**, 737 (2008).
- <sup>6</sup>C. A. Angell and I. S. Klein, *Nature Phys.* **7**, 750 (2011).
- <sup>7</sup>K. L. Ngai, *Relaxation and Diffusion in Complex Systems* (Springer, Berlin, 2011).
- <sup>8</sup>C. A. Angell, *Relaxations in Complex Systems*, edited by K. L. Ngai (Washington, DC, NRL, 1985), p. 3.
- <sup>9</sup>R. Böhmer, K. L. Ngai, C. A. Angell, and D. J. Plazek, *J. Chem. Phys.* **99**, 4201 (1993).
- <sup>10</sup>A. Drozd-Rzoska, S. J. Rzoska, and M. Paluch, *J. Chem. Phys.* **129**, 184509 (2009).
- <sup>11</sup>H. Tanaka, T. Kawasaki, H. Shintani, and K. Watanabe, *Nature Mater.* **9**, 324 (2010).
- <sup>12</sup>H. Vogel, *Phys. Z.* **22**, 645 (1921); G. S. Fulcher, *J. Am. Chem. Soc.* **8**, 339 (1925); G. Tammann and W. Hesse, *Z. Anorg. Allg. Chem.* **15**, 245 (1926).
- <sup>13</sup>A. K. Doolittle and D. B. Doolittle, *J. Appl. Phys.* **28**, 901 (1957).
- <sup>14</sup>R. J. Greet and D. Turnbull, *J. Chem. Phys.* **46**, 1243 (1967).
- <sup>15</sup>G. Adam, and J. H. Gibbs, *J. Chem. Phys.* **43**, 139 (1965).
- <sup>16</sup>F. Stickel, E. W. Fischer, and R. Richert, *J. Chem. Phys.* **104**, 2043 (1996).
- <sup>17</sup>C. Hansen, F. Stickel, P. Berger, R. Richert, and E. W. Fischer, *J. Chem. Phys.* **107**, 1086 (1997).
- <sup>18</sup>S. Corezzi, M. Beiner, H. Huth, K. Schröter, S. Capaccioli, R. Casalini, D. Fioretto, and E. Donth, *J. Chem. Phys.* **117**, 2435 (2002).
- <sup>19</sup>R. Casalini and C. M. Roland, *Phys. Rev. Lett.* **92**, 245702 (2004).
- <sup>20</sup>R. Casalini, M. Paluch, and C. M. Roland, *J. Chem. Phys.* **118**, 5701 (2003).
- <sup>21</sup>T. Blochowicz, C. Gainaru, P. Medick, C. Tschirwitz, and E. A. Rössler, *J. Chem. Phys.* **124**, 134503 (2006).
- <sup>22</sup>A. Drozd-Rzoska and S. J. Rzoska, *Phys. Rev. E* **73**, 041502 (2006).
- <sup>23</sup>J. C. Martinez-Garcia, J. Ll. Tamarit, and S. J. Rzoska, *J. Chem. Phys.* **134**, 024512 (2011).
- <sup>24</sup>T. Fujima, H. Frusawa, and K. Ito, *Phys. Rev. E* **66**, 031503 (2002).
- <sup>25</sup>V. N. Novikov and A. P. Sokolov, *Phys. Rev. E* **67**, 031507 (2003).
- <sup>26</sup>W. Kob, *Survey of Theories of Glass Transition*, lecture at School on Glass Formers and Glasses (Bengaulu, 2010); see <http://www.jncasr.ac.in/glassnotes/glasslectures/Kob/Walter-Kob-5Jan-Lecture2.pdf>.
- <sup>27</sup>R. Casalini and C. M. Roland, *Phys. Rev. B* **71**, 014210 (2005).
- <sup>28</sup>S. Bair, C. M. Roland, and R. Casalini, *Proc. Inst. Mech. Eng., Part J: J. Eng. Tribol.* **221**, 801 (2007).
- <sup>29</sup>C. M. Roland, *Soft Matter* **4**, 2316 (2008).
- <sup>30</sup>S. H. Chen, Y. Zhang, M. Lagi, S. H. Chong, P. Baglioni, and F. Mallamace, *J. Phys.: Condens. Matter* **21**, 504102 (2009).
- <sup>31</sup>L. O. Hedges, L. J. Robert, J. P. Garrahan, and D. Chandler, *Science* **323**, 1309 (2009).
- <sup>32</sup>F. Mallamace, C. Branca, C. Corsaro, N. Leone, J. Spooren, S.-H. Chen, and H. E. Stanley, *Proc. Natl. Acad. Sci. U.S.A.* **107**, 22457 (2010).
- <sup>33</sup>J. P. Garrahan, *Proc. Natl. Acad. Sci. U.S.A.* **108**, 4701 (2011).
- <sup>34</sup>H. Tanaka, *Phys. Rev. Lett.* **90**, 055701 (2003).
- <sup>35</sup>J. P. Eckmann and I. Procaccia, *Phys. Rev. E* **78**, 011503 (2008).
- <sup>36</sup>H. Bässler, *Phys. Rev. Lett.* **58**, 767 (1987).
- <sup>37</sup>I. Avramov, *J. Non-Cryst. Solids* **351**, 3163 (2005).
- <sup>38</sup>J. C. Mauro, Y. Yue, A. J. Ellison, P. K. Gupta, and D. C. Allan, *Proc. Natl. Acad. Sci. U.S.A.* **106**, 19780 (2009).
- <sup>39</sup>S. C. Waterton, *J. Soc. Glass Technol.* **16**, 244 (1932).
- <sup>40</sup>P. Lunkenheimer, S. Kastner, M. Köhler, and A. Loidl, *Phys. Rev. E* **81**, 051504 (2010).
- <sup>41</sup>H. C. Anderssen, *Proc. Natl. Acad. Sci. U.S.A.* **102**, 6686 (2005).
- <sup>42</sup>J. C. Martínez-García, Ph.D. dissertation, Technical University of Catalonia, Barcelona, 2011.
- <sup>43</sup>G. G. Naumis, *Phys. Rev. E* **71**, 026114 (2005).
- <sup>44</sup>P. K. Gupta and J. C. Mauro, *J. Chem. Phys.* **130**, 094503 (2009).
- <sup>45</sup>F. Stickel, E. W. Fischer, and R. Richert, *J. Chem. Phys.* **102**, 6251 (1995).
- <sup>46</sup>R. Richert and C. A. Angell, *J. Chem. Phys.* **108**, 9016 (1998).
- <sup>47</sup>A. Savitzky and M. J. E. Golay, *Anal. Chem.* **36**, 1627 (1964).
- <sup>48</sup>W. H. Press, S. A. Teukolsky, W. T. Vetterling, and B. P. Flannery, *Numerical Recipes: The Art of Scientific Computing*, 3rd ed. (Cambridge University Press, New York, 2007).
- <sup>49</sup>C. Zhang, L. Hu, Y. Yue, and J. C. Mauro, *J. Chem. Phys.* **133**, 014508 (2010).
- <sup>50</sup>M. Paluch, K. L. Ngai, and S. Hensel-Bielowka, *J. Chem. Phys.* **114**, 10872 (2001).
- <sup>51</sup>R. B. Bogoslovov, C. M. Roland, A. R. Ellis, A. M. Randall, and C. G. Robertson, *Macromolecules* **41**, 1289 (2008).
- <sup>52</sup>W. Heinrich and B. Stoll, *Colloid Polym. Sci.* **263**, 873 (1985).
- <sup>53</sup>F. Stickel, "Untersuchungen der dynamik in niedermolekularen Flüssigkeiten mit dielektrischer spektroskopie," Ph.D. dissertation (Mainz University, 1995).
- <sup>54</sup>R. Richert, *Physica A* **287**, 26 (2000).
- <sup>55</sup>C. M. Roland and R. Casalini, *J. Chem. Phys.* **122**, 134505 (2005).
- <sup>56</sup>S. Pawlus, K. Kunal, L. Hong, and A. P. Sokolov, *Polymer* **49**, 2918 (2008).
- <sup>57</sup>S. Corezzi, D. Fioretto, R. Casalini, and P. A. Rolla, *J. Non-Cryst. Solids* **307–310**, 281 (2002).
- <sup>58</sup>P. Lunkenheimer, R. Wehn, U. Schneider, and A. Loidl, *Phys. Rev. Lett.* **95**, 055702 (2005); R. Wehn, P. Lunkenheimer, and A. Loidl, *J. Non-Cryst. Solids* **353**, 3862 (2007).
- <sup>59</sup>C. M. Roland and R. Casalini, *J. Phys. Condens. Matter* **19**, 205118 (2007).
- <sup>60</sup>A. Drozd-Rzoska, S. J. Rzoska, S. Pawlus, J. C. Martínez-García, and J. Ll. Tamarit, *Phys. Rev. E* **82**, 031501 (2010).
- <sup>61</sup>A. Drozd-Rzoska, *J. Chem. Phys.* **130**, 234910 (2009).
- <sup>62</sup>A. Schönhals, *Europhys. Lett.* **56**, 815 (2001).
- <sup>63</sup>S. Pawlus, J. Bartos, O. Sausa, J. Kristiak, and M. Paluch, *J. Chem. Phys.* **124**, 104505 (2006).
- <sup>64</sup>A. Drozd-Rzoska, S. J. Rzoska, S. Pawlus, and J. Ll. Tamarit, *Phys. Rev. B* **73**, 224205 (2006).
- <sup>65</sup>J. C. Martínez-García, J. Ll. Tamarit, L. C. Pardo, M. Barrio, S. J. Rzoska, and A. Drozd-Rzoska, *J. Phys. Chem. B* **14**, 6099 (2010).
- <sup>66</sup>M. Köhler, P. Lunkenheimer, Y. Goncharov, R. Wehn, and A. Loidl, *J. Non-Cryst. Solids* **356**, 529 (2010).
- <sup>67</sup>R. Richert, F. Stickel, R. S. Fee, and M. Maroncelli, *Chem. Phys. Lett.* **229**, 302 (1994).
- <sup>68</sup>L. C. Pardo, P. Lunkenheimer, and A. Loidl, *J. Chem. Phys.* **124**, 124911 (2006).
- <sup>69</sup>D. Fragiadakis, R. Casalini, and C. M. Roland, *J. Phys. Chem. B* **113**, 13134 (2009).